

Supplementary Information of the Manuscript Entitled

Phosphorus-Doped Carbon-Carbon Nanotube Hierarchical Monoliths as True Three-Dimensional Electrodes in Supercapacitor Cells

by J. Patiño et al.

Figure S1. ^1H NMR spectrum of the DES formed between pTsOH·H₂O and TEP in a 1:1 molar ratio. See <http://www.sigmaaldrich.com/spectra/fnmr/FNMR011454.PDF> and http://www.chemicalbook.com/SpectrumEN_78-40-0_1HNMR.htm for comparison with the ^1H NMR spectrum of the individual components – e.g. pTsOH·H₂O and TEP, respectively.

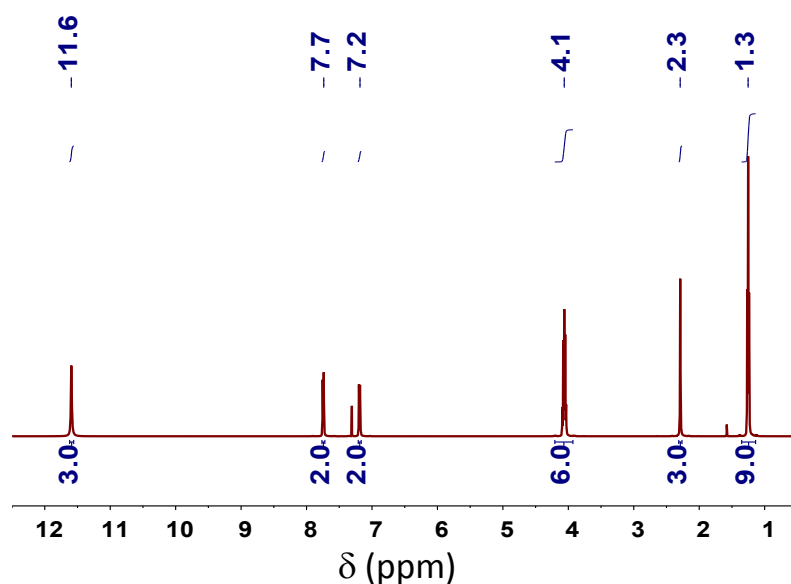


Table S1. Chemical shifts obtained from the ^1H NMR spectrum of the DES formed between pTsOH·H₂O and TEP in a 1:1 molar ratio and depicted in Figure S1. The chemical shifts of the individual components – e.g. pTsOH·H₂O and TEP – are also included for comparison.

Sample	δ (ppm)					
	p-Toluenesulfonic acid				Triethyl phosphate	
	H at C2	H at C3	H at SO ₃	H at CH ₃	H at C1	H at C2
pTsOH·H ₂ O	7.53	7.17	6.57	2.30		
TEP					4.11	1.35
Hydrated DES	7.74	1.78	11.59	2.29	4.06	1.25

STUDY OF DEGREE OF POLYCONDENSATION

In acidic aqueous solutions, condensation occurs via formation of either methylene (by condensation of a hydroxyl group of one furan with the C5-hydrogen of another) or methylene ether bridges (by condensation between the hydroxyl groups of two different furans), being the former more abundant than the latter. The influence (if any) that the use of a protic DES (rather than acidic water as solvent) has on the relative abundance of methylene and methylene ether groups was studied by FTIR and solid ^{13}C NMR spectroscopies. Thus, the signals at 816, 1176, 1353 and 3142 cm^{-1} in the FTIR spectrum were attributed to furan rings the signal at 781 to the bending out of plane of CH_2 linkage, and the signal 1561 cm^{-1} to the stretching of $-\text{C}=\text{C}-$ groups in 2-5 disubstituted furanic rings. Bands assigned to methylene (CH_2 groups) were also observed at ca. 2921 and 1443 cm^{-1} while that at 1010 cm^{-1} could be assigned to methylene ether groups (C-O benzyl ether groups). Solid state ^{13}C -CPMAS spectroscopy (Figure S3) provided useful information with regard to this issue as well. Thus, the peaks at ca. 22 ppm (assigned to methylene bridges), 111 ppm (assigned to C3 in furfuryl alcohol (FA) condensed via methylene bridges) and 149 ppm (assigned to C2 in FA condensed via methylene bridges) confirmed the preferred FA condensation via methylene bridges. The absence of the peak at 64 ppm assigned to methylene ether bridges further corroborated this issue.¹ Meanwhile, the peak at 129 ppm revealed that cross-linking of linear FA oligomers could also occur by the formation of $-\text{CH}_2-\text{O}-\text{CH}_2-$ linkages between the C3s or C4s of two furan rings. The three peaks at 44, 35, and 16 ppm were most likely due to mobile CH_3 groups in the resins.

¹ X. Zhang, D. H. Solomon, *J. Polym. Sci: Part B: Polym. Phys.* **1997**, *35*, 2233–2243

Figure S2. FTIR spectrum of the composite before carbonization at 800 °C.

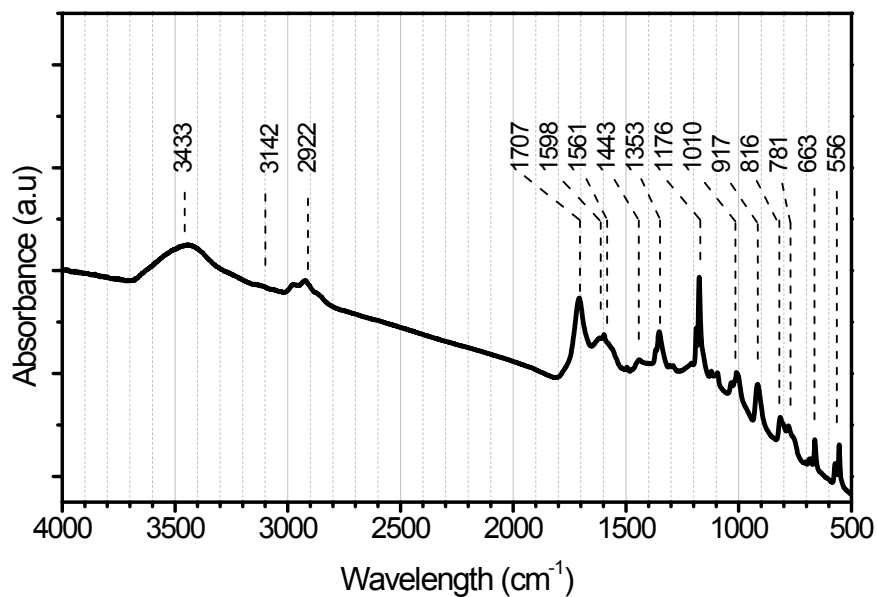


Table S2. Wavenumbers obtained from FTIR spectrum of the composite before carbonization at 800 °C.

$\nu(\text{cm}^{-1})$		$\nu(\text{cm}^{-1})$	
3433	OH	1176	Ring
3142	CH st from furfuryl	1010	C-O, from =CH-OH
2921	CH ₂	917	P ^v -O-C _{ar} st
1707	C=O st ar from furfury	816	Ring
1598	(COO) ⁻ st as	781	CH ₂ , δ oop
1561	-C=C-, 2-5 disubstituted furanic	663	PO ₃ ²⁻
1443	CH ₂ δ	556	PO ₄ ²⁻
1353	Ring		

Figure S3. Solid state ^{13}C -CPMAS spectrum of composite before carbonization at 800 °C. See reference 57 in the main text for comparison.

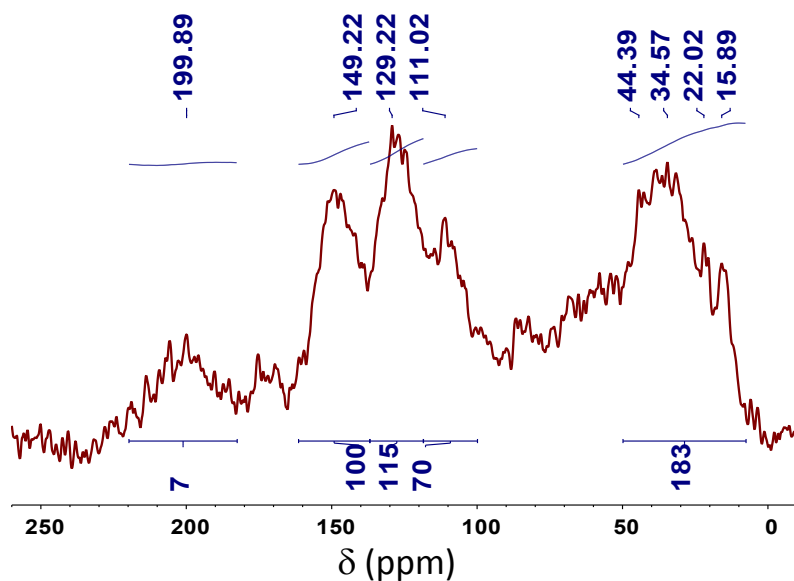


Figure S4. TGA (black lines) and DTA (blue lines) scans – carried out in oxygen – of the P-doped carbon-CNT composite (solid line) and of a P-doped carbon without CNTs (dotted line). This sample was included to better identify the temperature range where CNTs are burned out – e.g. 750-800 °C.

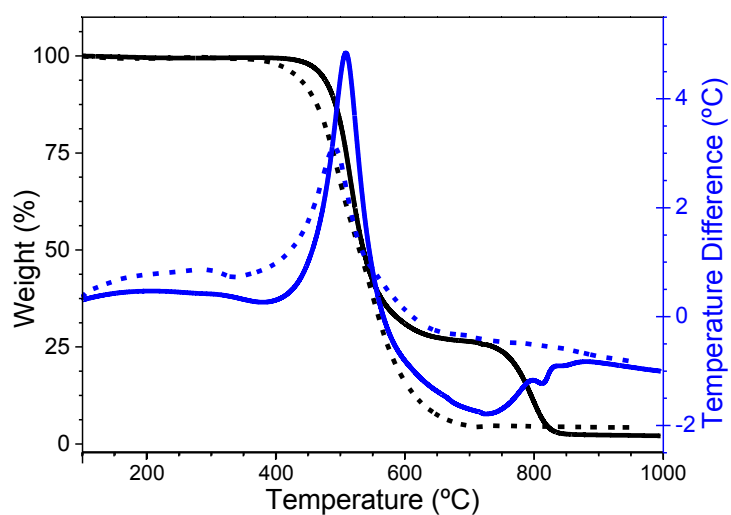


Figure S5. XRD pattern of the P-doped carbon-CNT composite.

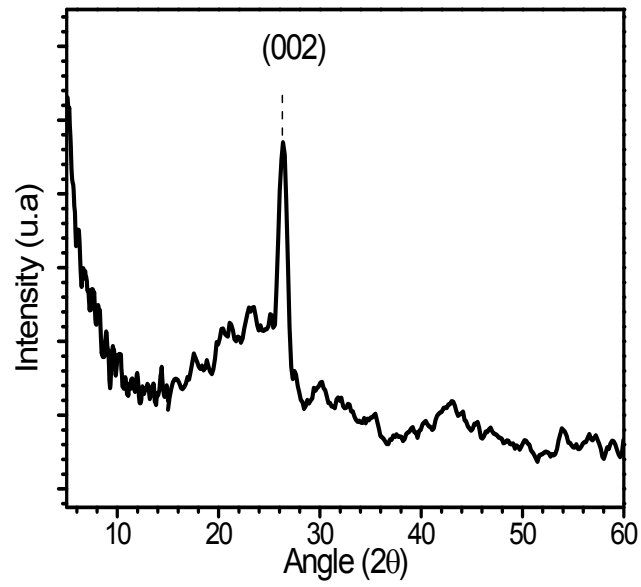


Figure S6. Pore size distribution obtained from the application of the 2D-NLDFT-HS method to N₂ adsorption/desorption isotherms.

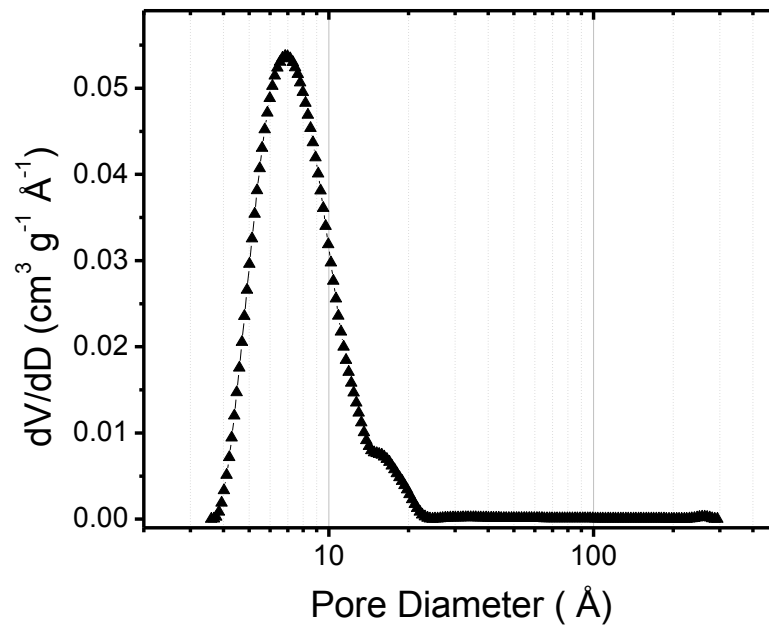


Figure S7. (a) Voltammogram of P-doped (black line) and non-doped (red line) carbon-CNT composites recorded at 5 mVs^{-1} in a Swagelok cell. (b) Voltammogram of the P-doped carbon-CNT composite recorded at 0.05 mVs^{-1} in a three-electrodes cell. The electrolyte was always H_2SO_4 2M.

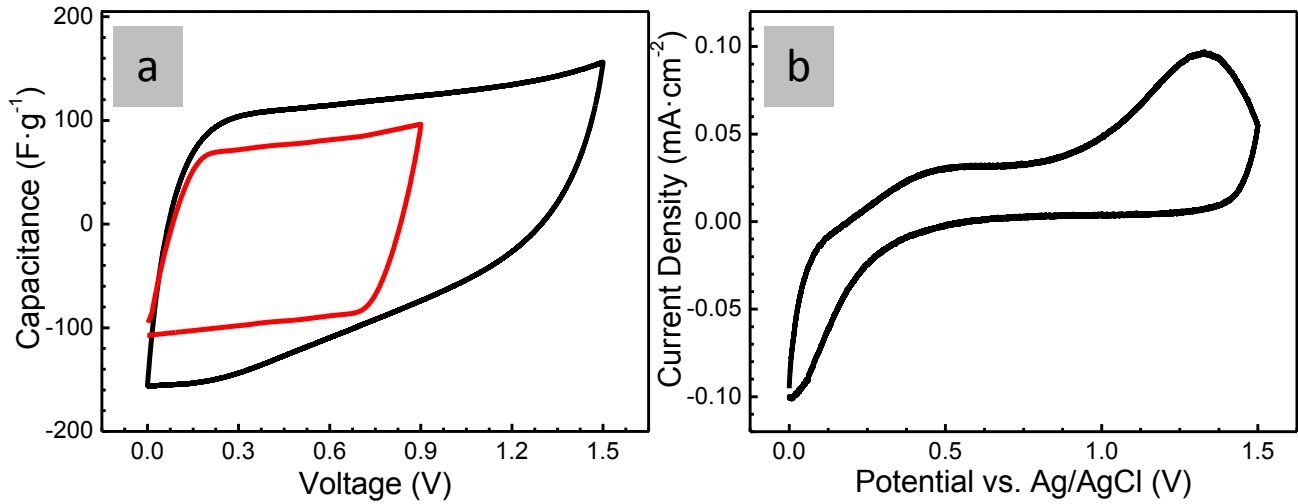


Figure S8. Nyquist (a) and Bode (b) plots of non-doped carbon-CNT composites obtained at different potentials for frequencies ranging from 0.01 to 10^5 Hz and an amplitude of 10mV.

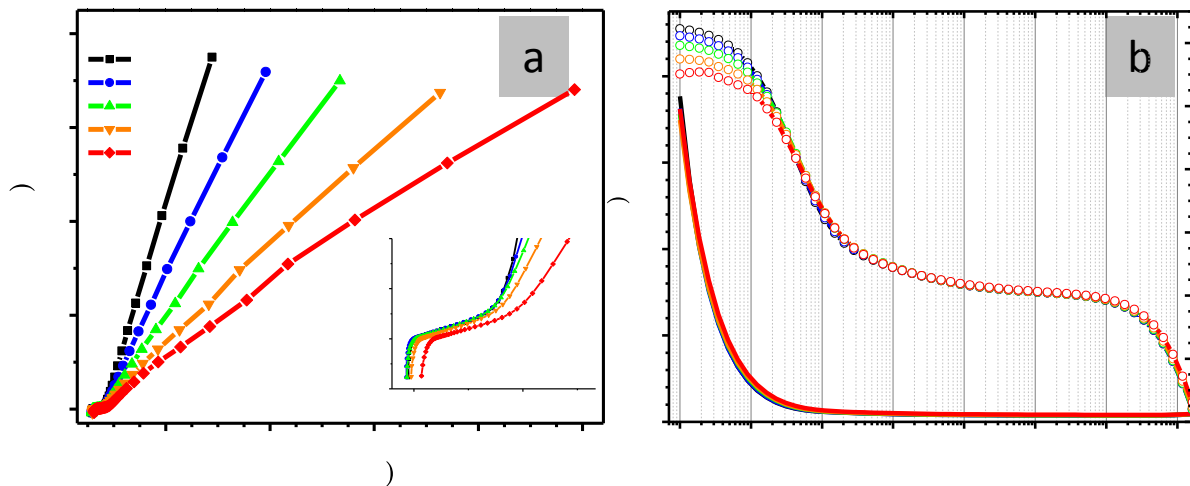


Table S3. Data obtained from N₂ (at 77 K, grey columns) and CO₂ (at 273 K, white columns) adsorption/desorption isotherms.

S_{BET} (m ² /g) ^a	Total volume (cm ³ /g) ^b	Micropore volume (cm ³ /g) ^c	Mesopore volume (cm ³ /g) ^c	L (nm) ^c	W_0 (cm ³ /g) ^d	W_0 (cm ³ /g) ^e	L (nm) ^f	E_0 (kJ/mol) ^e
937	0.411	0.351	0.025	0.68	0.371	0.237	0.62	28.9

^a Obtained after the application of the BET equation to the N₂ adsorption/desorption isotherm; ^b Obtained at $p/p_0 \approx 0.99$; ^c Obtained after the application of the 2D-NLDFT-HS method to the N₂ adsorption adsorption/desorption isotherm; ^d Obtained after the application of the Dubinin–Radushkevich equation to the N₂ adsorption adsorption/desorption isotherm; ^e Obtained after the application of the Dubinin–Radushkevich equation to the CO₂ adsorption adsorption/desorption isotherm; ^f Average narrow micropore size obtained after the application of the Stoeckli-Ballerini equation to the CO₂ adsorption/desorption isotherm.

Table S4. Phosphorus content as obtained from EDX-SEM, TXRF, and XPS.

Technique	Phosphorus content (wt%)
EDX	5.41
TXRF	4.31
XPS	6.27